Graduate Research in Engineering and Technology (GRET)

Volume 1
Issue 4 *Emerging Aerospace Technologies in Aerodynamics, Propulsion, and Materials.*

Article 6

January 2022

# Aerodynamic characteristics of owl like airfoil at low reynolds number

Ishfaq Fayaz
*Institute of aeronautical engineering*, ishfaqfayaz999@gmail.com

Syeda Needa Fathima
*Institute of aeronautical engineering*, syedaneedafathima12@gmail.com

Y D Dwivedi
*Institute of Aeronautical Engineering, Dundigal, Hyderabad*, yddwivedi@gmail.com



## Recommended Citation

Fayaz, Ishfaq; Fathima, Syeda Needa; and Dwivedi, Y D (2022) "Aerodynamic characteristics of owl like airfoil at low reynolds number," *Graduate Research in Engineering and Technology (GRET)*: Vol. 1 : Iss. 4 , Article 6.
DOI: 10.47893/GRET.2022.1054
Available at: https://www.interscience.in/gret/vol1/iss4/6

# Computational Study of Owl-Like Airfoil Aerodynamics at Low Reynolds Numbers In Forward Flight

*SYEEDA NEEDA FATHIMA*[1],*ISHFAQ FAYAZ*[1],*DR Y D DWIVEDI*[2]

*INSTITUTE OF AERONAUTICAL ENGINEERING, HYDERABAD, TELANGANA*

*DEPARTMENT OF AERONAUTICAL ENGINEERING*

## ABSTRACT

The computational investigation of aerodynamic characteristics and flow fields of a smooth owl-like airfoil without serrations and velvet structures.The bioinspired airfoil design is planned to serve as the main-wing for low-reynolds number aircrafts such as (MAV)micro air vechiles.The dependency of reynolds number on aerodynamics could be obtained at low reynolds numbers.The result of this experiment shows the owl-like airfoil is having high lift performance at very low speeds and in various wind conditions.One of the unique feature of owl airfoil is a separation bubble on the pressure side at low angle of attack.The separation bubble changes location from the pressure side to suction side as the AOA (angle of attack) increases. The reynolds number dependancy on the lift curve is insignificant,although there's difference in drag curve at high angle of attacks.Eventually, we get the geometric features of the owl like airfoil to increase aerodynamic performance at low reynolds numbers.

## KEYWORDS

Owl Wings, Low Reynolds Number, Aerodynamics, Separation Bubble

## 1. INTRODUCTION

Biomimetics includes the concepts and principles obtained from the nature for it's application in science and engineering such as in aerodynamic and fluid control devices. The serrated wing of the barn owl is an ideal example. Many studies have been found that by using a serrated design on the leading edge of an aircraft wing reduces aerodynamic noise [1] [2] [3].Moreover,the barn owl glides to hunt its prey at low reynolds number (approx. 30,000-90,000) based on the mean chord length of 180 mm [4].

In the past few years, the Flapping-wing Micro Aerial Vehicles (FMAVs) have attracted a lot of interest for their light weight, low flight noise, and high aerodynamic efficiency. In Comparison to the conventional fixed-wing flight, the flapping wing flight can offer many advantages in terms of energy consumption and flight agility. As far as the aerodynamic performances of FMAVs is concerned, it still has many limitations. The bird-like flapping wing cannot fly as efficiently or maneuverably as birds.

The aerospace community is interested in the low reynolds flight for developing (MAVs) [5] whose cruise reynolds number is in the order of O($10^4$). Liu et al [6] measured the surface geometry of various avian wings including owl wing by using a 3D laser scanner, to extract the wings geometrical properties including chamber line, thickness distribution , planform, chord distribution, and twist distributions. In comparison to other avian wings, the cross sectional shape of owl-like airfoil is a unique structure that is characterized by very thin wing thickness and high camber. Schmitz et al, described an airfoil that achieves high aerodynamic performance at low reynolds numbers [7] [8], which coincides with the geometric features of the owl wing.

This present study investigates the aerodynamic characteristics of an owl-like airfoil that approaches the flight reynolds numbers of an owl wing.however, unlike the actual owl wing that is characterized by serrations, a velvet and training-edge fringe structure and aeroelastically deformable feathers, the owl-like airfoil design of this study is solid and smooth. Konda et al [9] conducted 2D laminar analysis of the smooth owl-shape airfoil provided by Liu et al [6] at Re=23,000. They investigated the basic aerodynamic characteristics and flow fields around the airfoil and compared that with the ishii airfoil[10], which is considered as the pacemaker candidate for the main-wing airfoil of the japanese Mars airplane. However, the airfoil shape of their computational model is virtual since zero thickness is assumed in the vicinity of the trailing edge. Furthermore, a laminar separation is likely to occur with such a low Reynolds number along with the formation of a laminar separation bubble when the separated share layer transits from laminar to turbulent and reattaches to the surface. A behavior of the laminar separation bubble directly connects to the aerodynamic performance since it forms a strong negative pressure region on the surface and causes a nonlinear lift curve. Thus, the experimental investigations are required because the prediction accuracy of the reattachment point of the separation bubble is insufficient in the two-dimensional laminar analysis. The aim of the present work is to experimentally determine the Reynolds number dependency on the aerodynamic performance of an owl-like airfoil at low Reynolds numbers and to investigate the flow fields that leads to aerodynamic change using flow visualization.

## 2. METHODOLGY

### 2.1 OWL-LIKE AIRFOIL

The geometry of the test model airfoil in this study and that of the owl airfoil given by Liu et al [6] are compared in Fig 1.

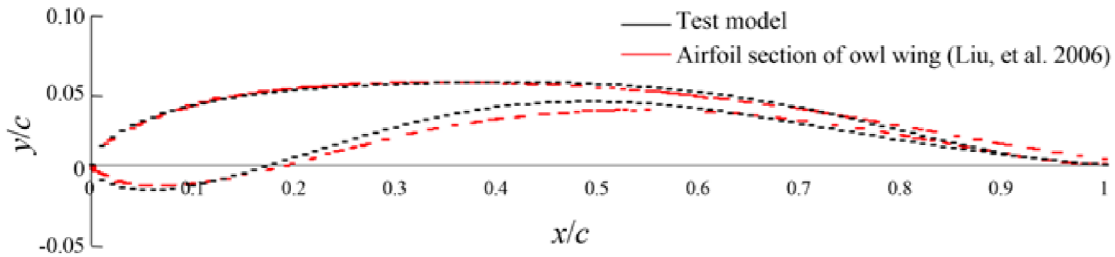


Fig 1.Airfoil section of owl-like wing (Black dash line:test model geometry,red dash line:Measured owl wing geometry).

The cross section of the owl airfoil (denoted by the red dash line) in Fig 1 is measured at 40% of the semi-span of the actual owl wing (2z/b = 0.4). The maximum airfoil thickness is as thin as 5.5% (t/c = 0.055) at x/c = 0.11. The wing thickness near the feathery trailing edge (x/c > 0.9) is zero. Since it is exceedingly difficult to create an airfoil model of this thickness dimension to withstand the wind tunnel test, a test model made of balsa wood with a thickness of 1.25% near the trailing edge, a chord length of 80 mm, and a span length of 180 mm was created.There were also slight differences in shape on the lower surface of the model (x/c = 0.2 - 0.6). The geometry of the test model, which is denoted by the black dash line in Fig 1, is measured using a noncontact three-dimensional laser scanning system.

### 2.2 COMPUTATIONAL APPROACH

Aerodynamic characteristics and flow fields around an owl-like airfoil at low reynolds numbers are investigated using 2D laminar flow computations. We generally use ANSYS FLUENT software for the analysis, in which we create the computational mesh around the owl-like airfoil and give the boundary conditions according to the dimensions of an aifoil and certain numerical equations are solved such as navier stokes equation.

## 2.3 METHOD:

- ✓ **DESIGN**

  The airfoil coordinates were extracted from the Lie et al[6] model by using the software GET DATA GRAPH DIGITIZER then these coordinates were imported in the PROFSCAN where geometry was made and we saved it as .DXF. Later, this file was imported in the CATIA V5 where geometry was modified (Fig 2) to do analysis and find the aerodynamic ratio's and airfoil characteristics.

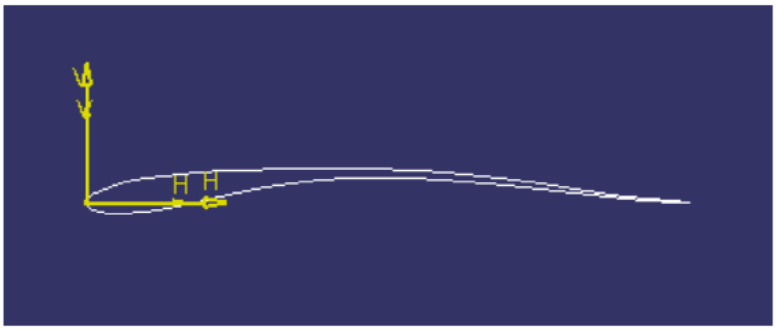


Fig 2**:** Owl-Like Airfoil In Catia

- ✓ **GEOMETRY**

  From CATIA, .stp file was imported in the geometry section in the fluent workbench and edited using design modeller. In design modeller the domain was created in which there was sufficient space from all the sides of an airfoil then by selecting the Name selection icon, we named all the boundaries and body as: Inlet, Outlet, Walls and Airfoil respectively.

- ✓ **MESHING**

  By doing the custom meshing we break down the domain into small number of pieces and each piece represents the element.
  As meshing is the process in which the continous geometry space of an object is broken down into thousands of shapes to properly define the physical shape of the object. Computational mesh around the owl-like airfoil is illustrated in Fig 3. Computational mesh contains 70959 Nodes and 69872 elements.
  Intially we did the body sizing by givng the size of each element as 5mm then we made the sphere of influence around the airfoil to capture all the flow characteristics near airfoil.later, we did edge sizing to control the upward flow near walls.lastly, we made inflation of 6 layers near edges of airfoil to capture the boundry layer separation more accurately. Finally we generate the mesh and it generates out as the desirable mesh.

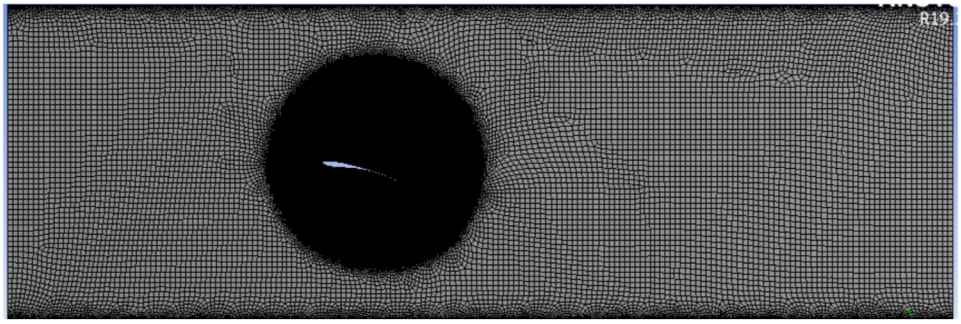

Fig 3 :mesh

- ✓ **SETUP AND SOLUTION**

  Once meshing is done, we do the fluent setup in which we check the mesh and give all the boundry conditions and give the inlet velocity. Moreover, we define the report definition of aerodynamic quantities. Moreover we intialize the fluent and in intialization we selected the standard intialization in which we compute from inlet and again gave the inlet velocity as 68.6 m/s. Eventually we run the calculations and got the desired solution.

- ✓ **RESULTS**

  In graphs we selected the contour, vectors, and pathlines and then plug the values. Various contours and vectors we got after plugging all the input conditions as you can check below in Fig 4, Fig 5, Fig 6 respectively.

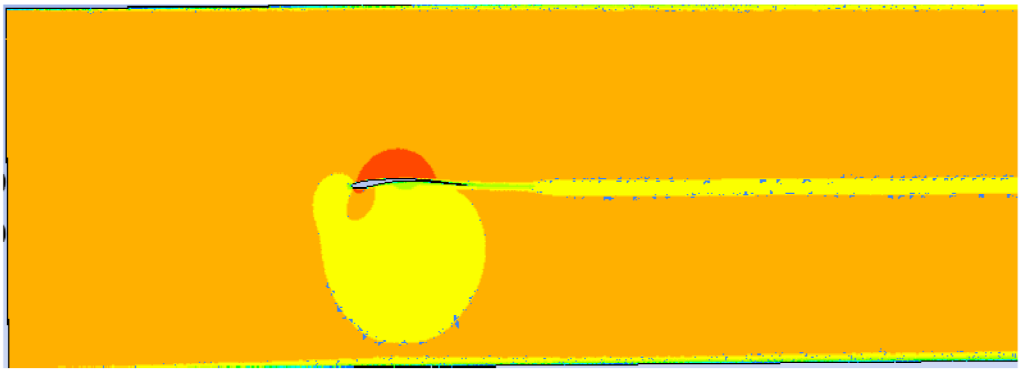

(a) velocity contour at $0^0$ α

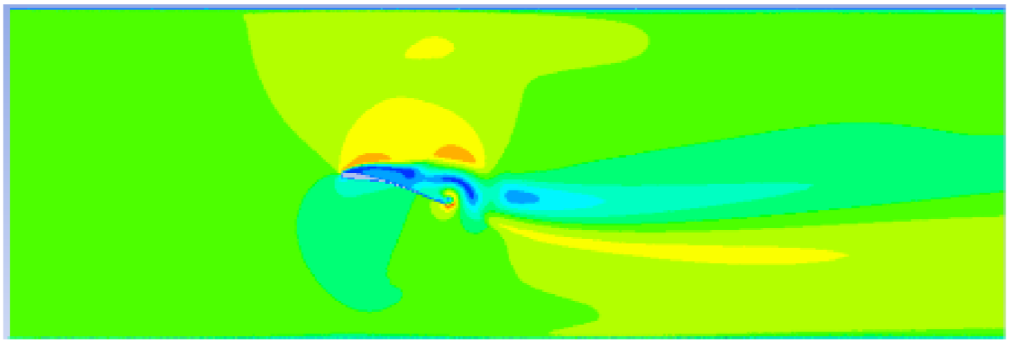

(b) at $16^0$ α

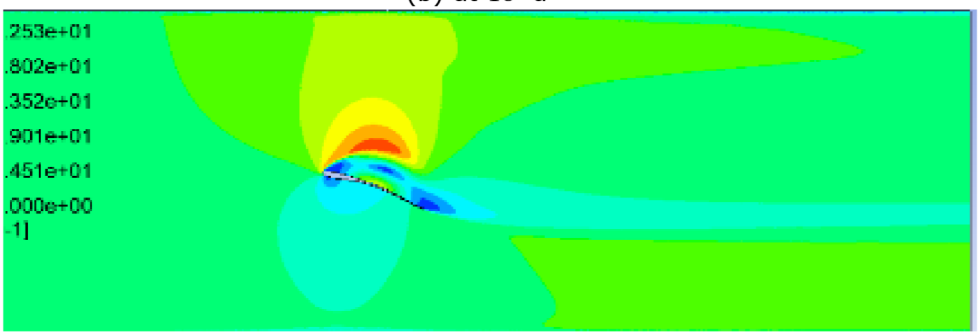


(c) at $24^0$ α

Fig 4: VELOCITY CONTOURS AT DIFFERENT α

In a, b ,c of Fig 4 we found that the at low α the flow remains attached and drag was pretty less. As we go on increasing the α (higher α) there was boundry layer separation which leads to vortex drag. However, it was less when we compared it to convention airfoils also there was much greater lift at low reynolds number apparently.

Similarly Fig 5 shows the turbulence contours at different α.

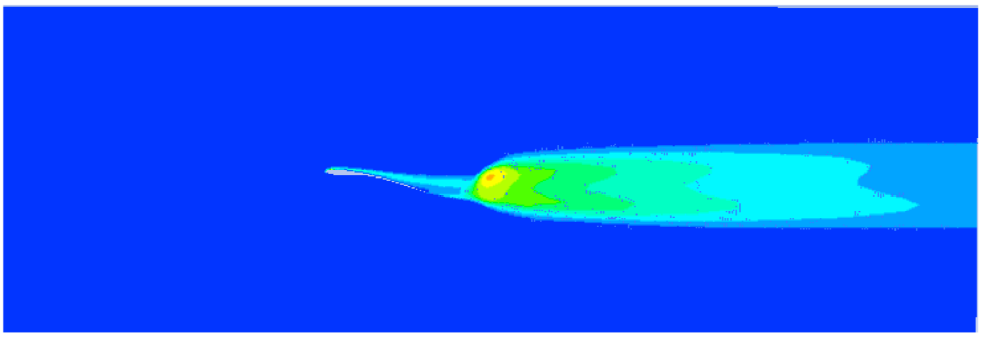

(a) at $4^0$ α

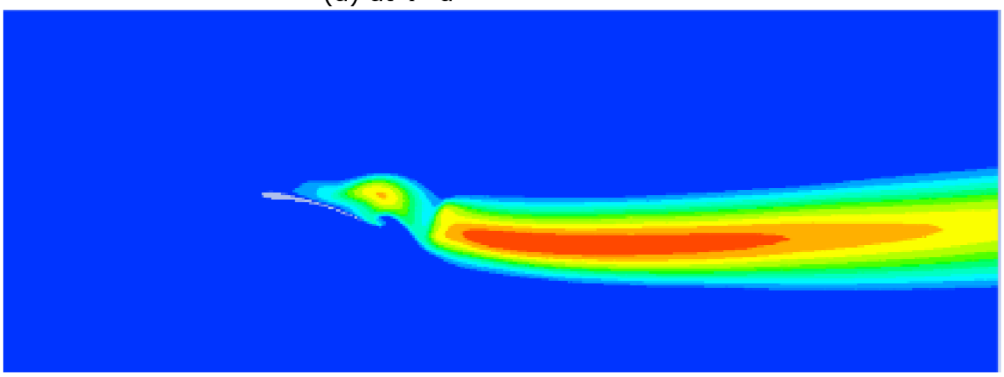

(b) at $16^0$α

Fig 5:TURBULENCE CONTOURS AT DIFFERENT α

As the velocity is not uniform throughout the airfoil thus, various directions and intensities of velocities you can found at different α.

The vectors in fig 6 shows clearly at low α, there were no reverse flow but as we go increasing α, we found that flow gets reverse at upper edge of airfoil.

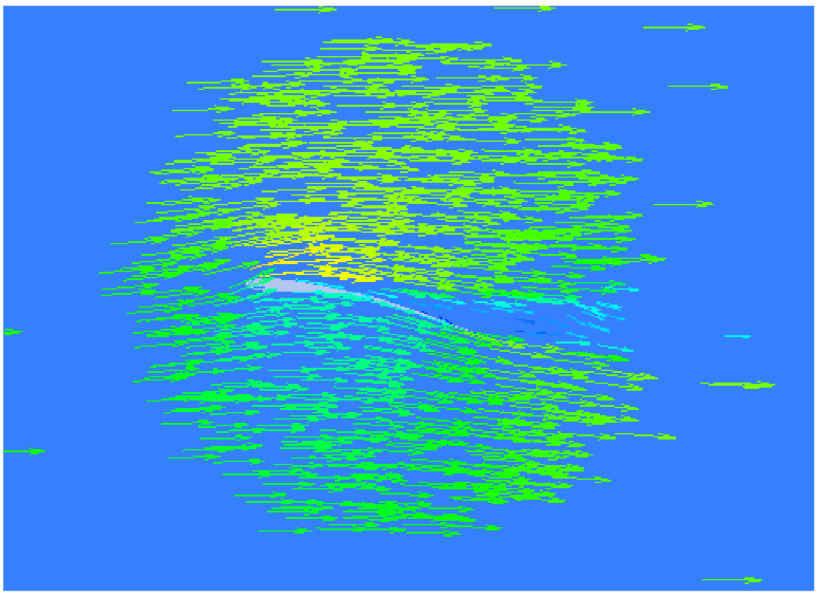

(a) at $4^0$ α

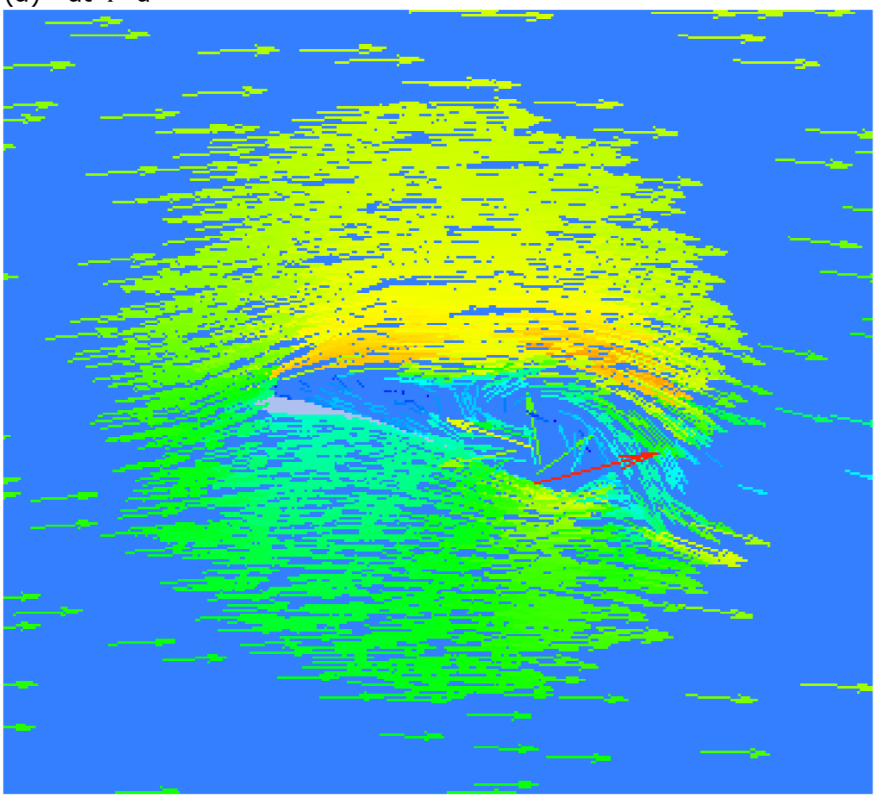

(b) at $16^0\alpha$

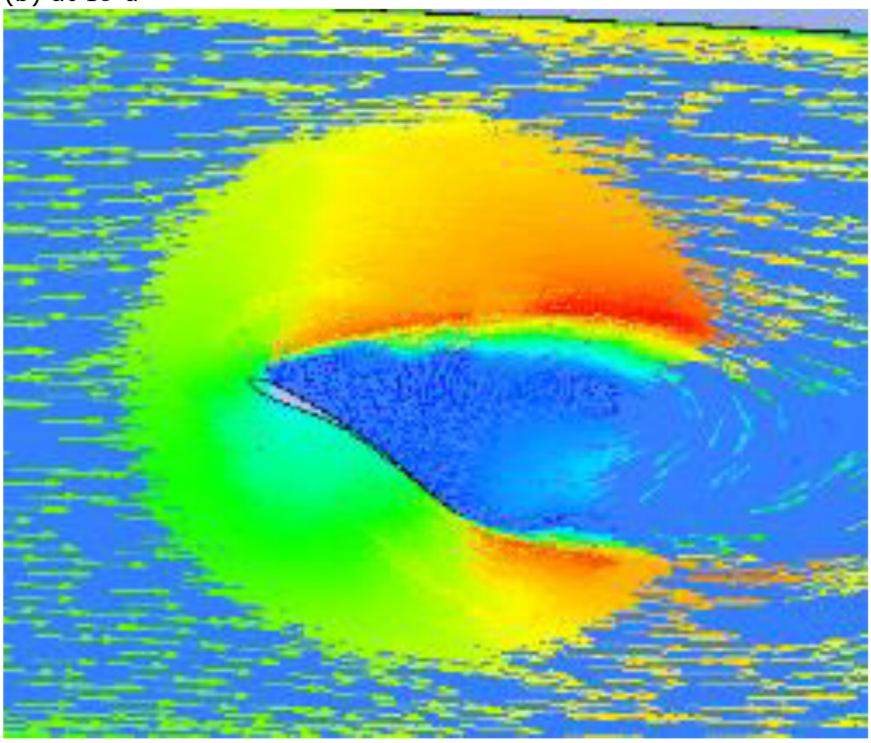

(c) at $30^0\alpha$

Fig 6: velocity vectors at different α

## 3. AERODYNAMIC CHARACTERISTICS

Fig 4 illustrates the aerodynamic force characteristics at Re=23,000. Lift coefficients and drag coefficients graphs are down below in Fig 7 (a), (b).

The computational results in fig 7 (a) shows lift variation at different angle of attacks (α) at the mach 0.2. we observed the Cl was increasing almost linearly at low angle of attacks from α=-4 deg to 4 deg. Although we observed slight difference at α = 5 deg. However, in conventional airfoils like NACA 0012 at low angle of attacks has lift curve lesser than owl-like airfoil. The lift coefficient reached almost the maximum value at α=17 deg.

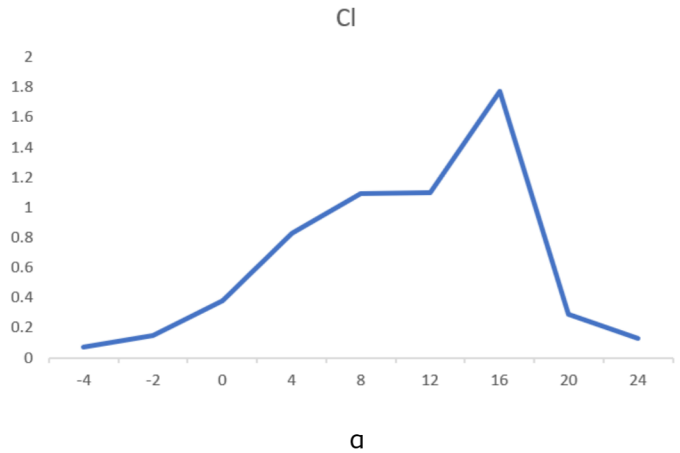


Fig 7 (a): lift coefficient vs angle of attack (α)

Also the computational results in fig 7 (b) shows the drag coefficient variations at different angle of attacks (α) at mach = 0.2 . the drag coefficient remains almost same till α = 4 deg. The difference in Cd was observed after the angle of attack α = 5 deg. The Cd reached to it's maximum value at α = 24 deg, moreover after α =24 deg the cl value decreased drastically.

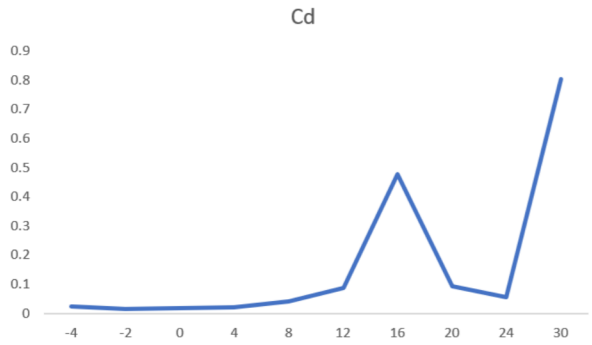


Fig 7 (b): drag coefficient vs angle of attack

### 3.1 NOMENCLATURE

b: Span Of Real Owl Wing

c: Chord Length

Cd: Coefficient Of Drag

Cl: Coefficient Of Lift

Re: Reynolds Number

α : Angle Of Attack

## 4. CONCLUSION

Due to the presence of deep concaved lower surface of owl-like airfoil and flat upper surface leads to more lift generation and drag reduction. The owl-like airfoil has higher lift to drag ratio than NACA 0012 airfoil at low reynolds number. At minimum drag, the lift coefficient of NACA 0012 airfoil become almost zero but the lift coefficient of owl-like airfoil doesn't. Owl-like airfoil generates more lift at low reynolds numbers since they have more cambered when compare to conventional airfoils. The flow remains almost laminar after the separation bubble in owl-like airfoil at low angle of attacks. The size of bubble depends upon the reynolds number and angle of attack. In owl-like airfoils the reynolds number dependency on lift curve is insignificant. At low angle of attacks, the flow on upper side and bottom side remains fully attached in the owl-like airfoil while in conventional airfoils it doesn't remain attached.

## 5. REFERENCES

[1] Alan, S.H., Paul, T.S. and Richard, E.H. (1974) Investigation of Acoustic Effects of Leading-Edge Serrations on Airfoils. Journal of Aircraft, 11, 197-202. https://doi.org/10.2514/3.59219

[2] Lilly, G.M. (1998) A Study of the Slight Flight of the Owl. 4th AIAA/CEAS Aeroacoustics Conference, AIAA Paper 98-2340, 1-6. https://doi.org/10.2514/6.1998–2340

[3] Wagner, H., Weger, M., Klaas, M. and Schröder, W. (2017) Features of Owl Wings that Promote Silent Fight. Interface Focus, 7, Article ID: 20160078. http://dx.doi.org/10.1098/rsfs.2016.0078

[4] Winzen, A., Klän, S., Klaas, M. and Schröder, W. (2012) Flow Field Analysis and Contour Detection of a Natural Owl Wing Using PIV Measurements. Nature-Inspired Fluid Mechanics: Results of the DFG Priority Programme 1207 "Nature-Inspired Fluid Mechanics" 2006-2012. Springer, Berlin, 119-134. https://doi.org/10.1007/978-3-642-28302-4_7

[5] Mueller, T.J., Kellogg, J.C., Ifju, P.G. and Shkarayev, S.V. (2007) Introduction to the Design of Fixed-Wing Micro Air Vehicles: Including Three Case Studies. AIAA Education Series, Reston. https://doi.org/10.2514/4.862106

[6] Liu, T., Kuykendoll, K., Rhew, R. and Jones, S. (2006) Avian Wing Geometry and Kinematics. AIAA Journal, 44, 954-963. https://doi.org/10.2514/1.16224

[7] Schmitz, F.W. (1976) Aerodynamic of the Model Airplane Part 1. NASA TM-X-60976.

[8] Schmitz, F.W. (1980) The Aerodynamics of Small Reynolds Number. NASA TM-51

[9] Kondo, K., Aono, H., Nonomura, T., Anyoji, M., Oyama, A., Liu, T., Fujii, K. and Yamamoto, M. (2014) Analysis of Owl-like Airfoil Aerodynamics at Low Reynolds Number Flow. Transactions of the Japan Society for Aeronautical and Space Sciences, 12, Tk 35-Tk 40. https://doi.org/10.2322/tastj.12.Tk_35

[10] Anyoji, M., Nonomura, T., Aono, H., Oyama, A., Fujii, K., Nagai, H. and Asai, K. (2014) Computational and Experimental Analysis of a High-Performance Airfoil under Low-Reynolds-Number Flow Condition. Journal of Aircraft, 51, 1864-1872. https://doi.org/10.2514/1.C032553